Available online at www.sciencedirect.com
ScienceDirect
Trans. Nonferrous Met. Soc. China 31(2021) 999−1011
Transactions of Nonferrous Metals Society of China
www.tnmsc.cn

Electrochemical response of Ti joints vacuum brazed with TiCuNi, AgCu, and Ag fillers

C. MARINHO[1], F. TOPTAN[1,2], A. GUEDES[1,3], A. C. ALVES[1]

1. CMEMS-UMinho, Center of MicroElectroMechanical Systems, University of Minho, Guimarães, Portugal;
2. IBTN/Euro, European Branch of the Institute of Biomaterials, Tribocorrosion and Nanomedicine, Department of Mechanical Engineering, University of Minho, Guimarães, Portugal;
3. Department of Mechanical Engineering, University of Minho, Guimarães, Portugal

Received 15 April 2020; accepted 19 October 2020

Abstract: The properties of the joints are dictated by the nature, distribution, and morphology of the phases formed at the interface. The mechanical properties of brazed joints are well documented in the literature, contrarily to their electrochemical behaviour. Thus, the main objective of this study was to understand the influence of the phases formed at the interface on the corrosion behaviour of commercially pure Ti brazed joints, produced by using TiCuNi, eutectic AgCu, and Ag filler foils. The electrochemical behaviour of the Ti joints was accessed by open circuit potential and potentiodynamic polarization tests in phosphate buffer saline solution electrolyte at body temperature. Results showed that Ag-based fillers induced susceptibility to micro-galvanic corrosion between the Ag-rich and Ti phases formed at the interface and commercially pure Ti base metal. However, no significant differences were observed between the joint system and the base material when brazing with TiCuNi filler.

Key words: biomaterial; titanium; joining; brazing alloys; interface; microstructure; corrosion

1 Introduction

Commercially pure (cp) Ti presents a number of desirable properties for several applications as relatively low density, good corrosion resistance, and biocompatibility [1−3], making it an ideal material for biomedical implant applications. The fabrication of biomedical implants may require the joining of multiple simple parts in order to simplify the production with low cost. Joining can be achieved by several techniques, such as welding, diffusion bonding, and brazing. Welding Ti presents several challenges related to the high melting point and affinity of Ti towards oxygen, hydrogen or nitrogen, requiring careful control of the process in order to minimize the formation of defects and brittle phases, the development thermally induced stresses, and the extent of the heat affected zone. In fact, due to the diffusion of oxygen during the processes of melting or welding, Ti tends to become brittle, and may undergo microstructural alterations that may degrade its mechanical properties [4−10]. In addition, modification occurring on the microstructure of Ti and its alloys at the heat affected zones may change locally the characteristics of the natural oxide film formed on the Ti surfaces [11−15].

Brazing techniques have been used for 5000 years since ancient Egyptians and Sumerians as they are relatively low-cost, simple, and versatile joining procedures [16]. Brazing allows to produce parts with complex geometries by joining simple parts, at relatively low processing temperatures and without the need of applying elevated joining pressures to promote bonding, thus minimizing the

Corresponding author: A. C. ALVES; Tel: +351-253510220; Fax: +351-253516007; E-mail: alexandra@dem.uminho.pt
DOI: 10.1016/S1003-6326(21)65556-5

degradation of the base materials as the result of the joining procedure. According to a recent review by WAY et al [16], brazing techniques are classified as flame brazing, induction brazing, and furnace/ vacuum brazing. Among these, vacuum brazing is reported to be a straightforward process to join metals having very stable oxide films, such as Ti [16]. The mechanical behaviour of vacuum brazed joints is well documented in Refs. [17−26] and is highly dependent on the nature of the phases that are formed at the brazing interface.

Although presenting adequate mechanical strength, the degradation behaviour at brazing interface may limit the operating life time of brazed joints, depending on the service environment [27]. Even so, the influence of interfacial reaction products on the corrosion behaviour of the joints is still scarce [18,27−29]. Galvanic corrosion or dealloying can be observed at the brazing interface, which may also provide suitable spots for the initiation of pitting corrosion. For instance, KVRYAN et al [27] studied the micro-galvanic corrosion behaviour of 316L stainless steel brazed with AgCuTi and AgCuInTi fillers by scanning Kelvin probe force microscopy (SKPFM) analysis, in order to obtain Volta potential difference maps. They reported that the Volta potential was more negative on the base materials as compared to the interfacial reaction products, leading to formation of galvanic couples, and consequently, to the micro-galvanic corrosion. KIM et al [30] brazed Zircaloy-4 using Zr-rich brazing alloys and reported the micro-galvanic corrosion as the dominant corrosion mechanism occurring due to coupling of α-Zr grains containing Ti and the base metal. ELREFAEY et al [31] joined cp Ti to low carbon steel with a Cu-based filler and reported that the filler metal (Cu−10.6Mn−1.9Ni, at.%.) led to a severe galvanic corrosion on steel in 0.1 mol/L sulfuric acid. BENEDETTI et al [32] studied the Ti6Al4V−$Y_3Al_5O_{12}$ joints brazed with Ag and AgCu fillers and reported Cu depletion at the brazing interface in seawater, when AgCu filler was used. On the other hand, LEE et al [33] joined Ti with ZrTiNiCuBe bulk metallic glass brazing filler and reported pitting corrosion in 3.5 wt.% NaCl solution, of joints brazed at 780 °C, at the central zone of interface where Zr–Cu–Ni segregation occurred. Apart from the influence of incorporating filler metal elemental species that diffuse and dissolve into the base materials in the course of joining, the brazing thermal cycle can even cause pitting corrosion for some metals, as reported by KVRYAN et al [27]. They observed significantly low pitting potential and linked this behaviour with grain boundary sensitization, which was promoted by the brazing thermal cycle. Nevertheless, some authors [34] reported the corrosion behaviour of the Ti−B_4C joints brazed with TiCuNi filler alloy, where no negative effect on the corrosion behaviour was detected in 0.9 wt.% NaCl solution.

Before considering their use in biomedical applications, the effect of the brazing filler metals on the corrosion behaviour of the brazed joints needs to be assessed. Thus, this work aimed to study the influence of brazed interface on the corrosion behaviour of cp Ti joined by brazing using TiCuNi, eutectic AgCu, and Ag filler foils intended to be used in biomedical applications.

2 Experimental

Ti samples (12 mm in diameter, 3 mm in thickness) were processed by powder metallurgy using angular shaped Ti powders having an average size of 36 μm (Grade 2, Alfa Aesar) together with PVA (0.4 vol.%) as binder. Ti powders and PVA were mixed in a ball mill rotating at 130 r/min and under Ar atmosphere for 4 h with Al_2O_3 balls. After mixing, the blended powders were uniaxially pressed in a nitrided stainless steel die lubricated with zinc stearate, for 2 min at 350 MPa. The binder removal was performed at 450 °C for 3 h in Ar atmosphere, followed by sintering at 1100 °C for 3 h in a high vacuum (<1 mPa) horizontal tubular furnace.

Ti joints were produced by brazing using different commercial fillers foils, which will be designated hereafter as TiCuNi (Ti−15Cu−15Ni, wt.%, 90 μm in thickness), AgCu (Ag−28Cu, wt.%, 100 μm in thickness) and Ag (99.96 wt.% Ag, 125 μm in thickness). The brazed Ti joints were obtained by fixing the brazing assemblage (Ti/brazing filler/Ti) in a stainless-steel holder and placed it in a high vacuum tubular furnace (<1 mPa). Samples were heated to the brazing temperature at a rate of 5 °C/min, followed by a dwelling stage of 30 min and then cooled to room temperature at 5 °C/min. Table 1 lists, for each of the selected brazing fillers, the minimum processing

temperature that induced the formation of sound joints, i.e., joints apparently free of pores, cracks, and unbonded zones.

Table 1 Liquidus/melting and minimum brazing temperatures for producing sound joints with each brazing filler, together with corresponding joint identification

Brazing alloy	Liquidus temperature/ °C	Brazing temperature/ °C	Joint identification
TiCuNi	960	1000	Ti/TiCuNi/Ti
Ag	960	1100	Ti/Ag/Ti
AgCu	780	810	Ti/AgCu/Ti

For the microstructural characterization and electrochemical tests, cross-sections of brazed joints were cut with a diamond disk and ground with SiC paper down to 2.1 μm. For microstructural and chemical analysis, the cross-section surfaces were polished down to 1 μm diamond suspension finishing. After metallographic preparation, samples were cleaned by ultrasounds sequentially for 10 min in propanol and 5 min in distilled water.

All electrochemical tests were performed immediately after sample preparation, at body temperature ((37±2) °C), in phosphate buffer saline solution (PBS: 0.2 g/L KCl, 0.24 g/L KH_2PO_2, 1.44 g/L Na_2HPO_4, 8 g/L NaCl). Before the electrochemical tests, the pH of PBS electrolyte was measured (EUTECH Instruments pH 510) and adjusted to 7.4±0.1. Open circuit potential (OCP) and potentiodynamic polarization test were performed by using a potentiostat (Gamry Instruments Reference 600^+ Potentiostat/ Galvanostat/ZRA), where the samples were connected as the working electrode, having an exposed area to the electrolyte of 0.38 cm^2, a saturated Ag/AgCl electrode was used as the reference electrode, and a Pt wire was connected as the counter electrode. OCP was monitored at least for 90 min to stabilize the system and the last 10 min of immersion was recorded. The potentiodynamic scans were performed in the anodic direction starting from −0.25 V(OCP) till 1.5 V(Ag/AgCl) at a scanning rate of 0.5 mV/s. In order to ensure repeatability of results, each test was repeated at least 3 times and the results are given as average ± standard deviation. After the potentiodynamic polarization tests, the corroded surfaces were cleaned with the same procedure described above. The microstructure and the chemical composition of the as-brazed and corroded interfaces were analysed by scanning electron microscopy (SEM) and energy dispersive spectroscopy (EDS).

3 Results and discussion

3.1 Microstructural characterization and chemical composition

3.1.1 Ti/TiCuNi/Ti joints

Figure 1 presents the SEM images of Ti/TiCuNi/Ti brazed joints. The reaction between the filer and cp Ti led to the formation of an extensive interface composed of two layers, with a total thickness of about 580 μm which is more than six times the thickness of the brazing filler foil (90 μm). Layer A is around 280 μm in thickness and corresponds to the central zone of the interface. Layer B extends from Layer A into the base cp Ti samples and presents a width of about 150 μm. Layer B presents a similar microstructure to cp Ti, but it is enriched in Cu and Ni (up to 1.5 at.% each) that diffused from the TiCuNi filler. Thus, Layer B could be described as a diffusion zone on cp Ti samples.

The heating and cooling rates used in this work were slow enough, to reasonably assume that a quasi-equilibrium state was achieved at the interface during the entire thermal cycle. Thus, the equilibrium phase diagram together with the SEM images and EDS analysis can be used to predict the nature of the phases presented at the interface [35,36]. The same approach will be used for the other two brazing systems analysed in this study. Since Ti/TiCuNi/Ti brazed joint interface was mostly composed of Ti, Cu, and Ni, the Ti−Cu−Ni ternary equilibrium phase diagram (Fig. 1(c)) was selected to predict the nature of the interfacial reaction products. Accordingly, Table 2 presents the EDS analysis results together with the possible phases formed at the interface.

Three different zones could be observed in Layer A, each composed of different constituents/ phases (Fig. 1(b)), namely, a coarse grey phase (Zone 1 in Fig. 1(b) and Table 2), a lamellar constituent (Zone 2 in Fig. 1(b) and Table 2), and a thin light grey phase (Zone 3 in Fig. 1(b) and Table 2). The coarse grey phase was composed of

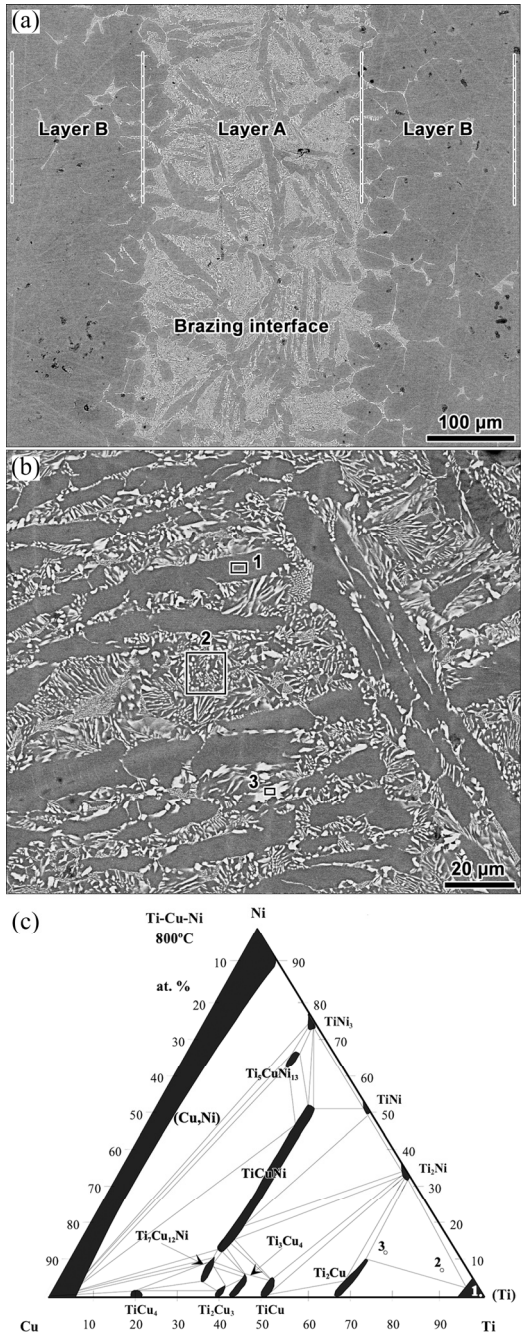

Fig. 1 Backscattered electron (BSE) images of Ti/TiCuNi/Ti brazed joints showing global view (a), microstructure of brazing interface (b), and isothermal section of TiCuNi phase diagram at 800 °C (c) [35]

Table 2 Chemical composition of different zones shown in Fig. 1(b)

Zone	Composition/at.%			Possible phase
	Ni	Ti	Cu	
1	0.6	98.2	1.2	α-Ti
2	4.0	90.1	5.9	α-Ti+(Cu,Ni)Ti_2
3	10.6	71.7	17.7	(Cu,Ni)Ti_2

more than 98 at.% Ti, and its chemical composition on the isothermal section of Ti−Cu−Ni phase diagram (Fig. 1(c)) indicates that it should be α-Ti with some dissolved Cu and Ni. The thin light grey phase was rich in Ti, Cu, and Ni, and its chemical composition was on the (Cu,Ni)Ti_2 narrow strip single phase field on the isothermal section of the phase diagram. Therefore, this phase should be the (Cu,Ni)Ti_2 intermetallic compound. Accordingly, the lamellar constituent can be interpreted as a mixture of α-Ti and (Cu,Ni)Ti_2. These results are in accordance with Refs. [2,34,37] on the brazing of Ti-based materials using TiCuNi as filler alloy. For instance, GOMES and GUEDES [37] studied the joining of Ti6Al4V, using TiCuNi as brazing alloy. The resulting interface presented an extensive diffusion layer around 330 μm. Moreover, they also suggested that the observed Widmanstätten morphology was composed of α-Ti plates delimited by (Cu,Ni)Ti_2 intermetallics. On the other hand, some authors [34] used TiCuNi as brazing alloy to join Ti−B_4C composites and reported an interface presenting about 400 μm of thickness consisting of two different layers, i.e., a central zone (about 200 μm) and a diffusion layer extending into the base material. Moreover, the central zone was reported to exhibit four distinct constituents, namely, α-Ti, (Cu,Ni)Ti_2, a lamellar constituent, and undissolved B_4C reinforcement particles. The lamellar constituent was assumed to consist of a mixture of α-Ti and (Cu,Ni)Ti_2 intermetallic. CHANG et al [2] used Ti−15Cu−15Ni and Ti−15Cu−25Ni fillers to join cp Ti by infrared vacuum brazing and reported that the brazed interface consisted of Ti_2Cu/Ti_2Ni intermetallic compounds and a Ti-rich matrix. SHIUE et al [38] produced infrared brazed α_2-Ti_3Al/Ti−6Al−4V joints using Ti−15−Cu−25Ni and Ti−15Cu−15Ni as filler metals. They concluded that the interfaces were composed, essentially, of a Ti-rich matrix and Ti_2Ni phase.

3.1.2 Ti/Ag/Ti joints

Figure 2 shows SEM images of Ti/Ag/Ti brazed joints and Table 3 presents the chemical compositions of the different zones marked in Fig. 2(b). The Ti/Ag/Ti interface is composed of two layers and is around 420 μm, which is more than three times the thickness of Ag foil (125 μm). The large extension of the interface denotes that an intense reaction occurred between the Ag filler foil

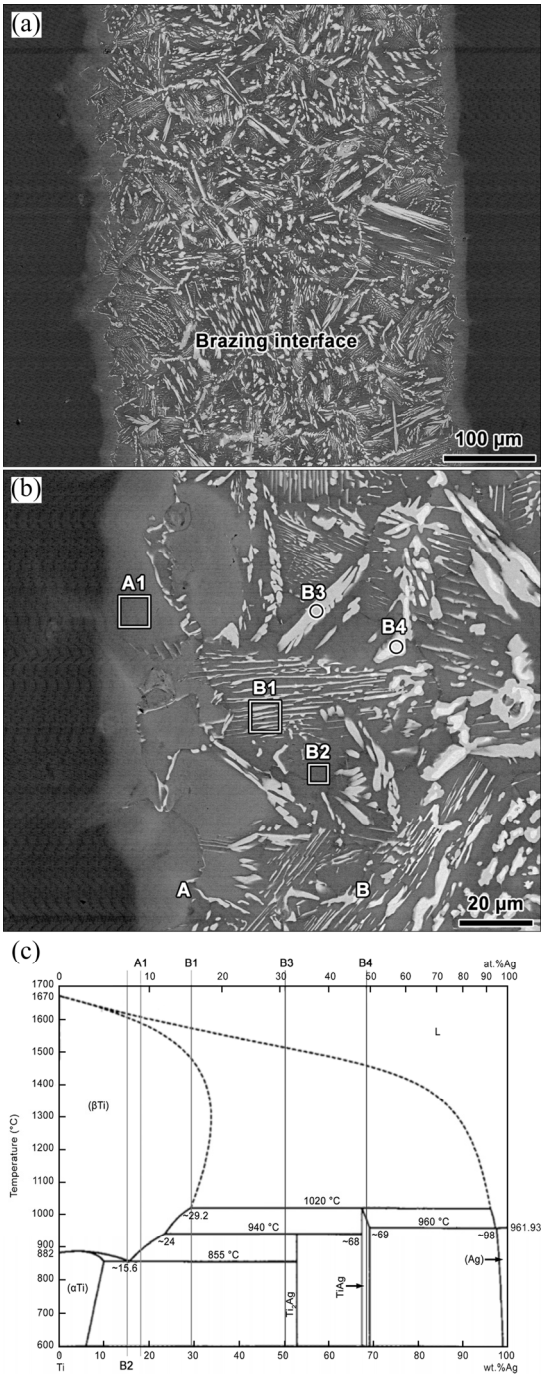

Fig. 2 BSE images of Ti/Ag/Ti brazed joints showing global view (a), microstructure of brazing interface (b), and Ti−Ag phase diagram (c) [39]

and cp Ti samples. The reaction was enhanced by the high processing temperature (1100 °C) required to produce sound Ti/Ag/Ti brazed joints.

Layer A (about 10 μm) is observed adjacently to the Ti base material and is composed of more than 90% of Ti and should result from the diffusion of Ag into the cp Ti samples. The typical chemical composition of zones analysed in Layer A, is marked on the Ag−Cu equilibrium phase diagram presented in Fig. 2(c) [39]. The composition of zone (A1) is located on the α-Ti+Ti_2Ag two-phase field, but close to the α-Ti single phase domain. Therefore, it is reasonable to assume that Layer A should be mainly composed of α-Ti. Layer B (about 400 μm) is composed of a mixture of bright (B3 and B4), dark (B2), and lamellar (B1) zones. According to the EDS analysis results presented in Table 2 and the Ag−Cu equilibrium phase diagram, the dark zones should be α-Ti, the bright zones, B3 and B4, are probably Ti_2Ag and TiAg intermetallics, respectively, and the lamellar zones are a mixture of α-Ti and Ti_2Ag. Thus, considering these results, it is possible to assume that the following sequence of phases is present at the brazing Ti/Ag/Ti interface, from the centre of the interface towards cp Ti samples: TiAg+Ti_2Ag+α-Ti (Layer B)/α-Ti (Layer A).

Table 3 Chemical composition of different zones shown in Fig. 2(b)

Layer	Zone	Composition/at.%		Possible phase
		Ag	Ti	
A	A1	9.0	91.0	α-Ti
B	B1	15.5	84.5	α-Ti+Ti_2Ag
	B2	7.5	92.5	α-Ti
	B3	30.9	69.1	Ti_2Ag
	B4	49.5	50.5	TiAg

Ti−Ag intermetallics, (Ti) and (Ag) are often reported at interfaces resulting from joining Ti or its alloys when Ag is used as filler. For instance, SHIUE et al [40] reported that the TiAl/Ag/TiAl infrared brazed interface consisted of (Al,Ag)Ti, (Al,Ag)Ti_3 and (Ag). DENG et al [41] studied the diffusion bonding of Ti/stainless steel joints using Ag interlayer as filler. The Ti/Ag interface was characterized as presenting a diffusion zone and a reaction layer, consisting of (Ti) and TiAg, respectively. In addition, (Ag) remaining from the filler foil was also detected at the centre of the interface. WANG et al [42] joined Ti to 304 stainless steel by electron beam welding using different fillers. For Ti/Ag/stainless steel joints processed with Ag filler, the interface was inferred to be composed of a Ti_2Ag reaction layer. Recently, YU et al [43] showed electron beam welded Ti6Al4V joint interface, using Ag interlayer, was composed of (Ti), (Ag), and a small amount of Ti_2Ag.

3.1.3 Ti/AgCu/Ti brazed joints

SEM images of Ti/AgCu/Ti brazed joints and the chemical composition of the different zones detected at the interface are presented in Fig. 3 and Table 4, respectively. A multilayered interface, with a thickness of around 125 μm, composed of four distinct layers, marked in Fig. 3(b) as A, B, C and D, was observed. Layer A, which is detected at the centre of the interface (Fig. 3(b)), is about 110 μm in thickness and composed of a mixture of dark (A1) and a light grey (A2) zones. According to the

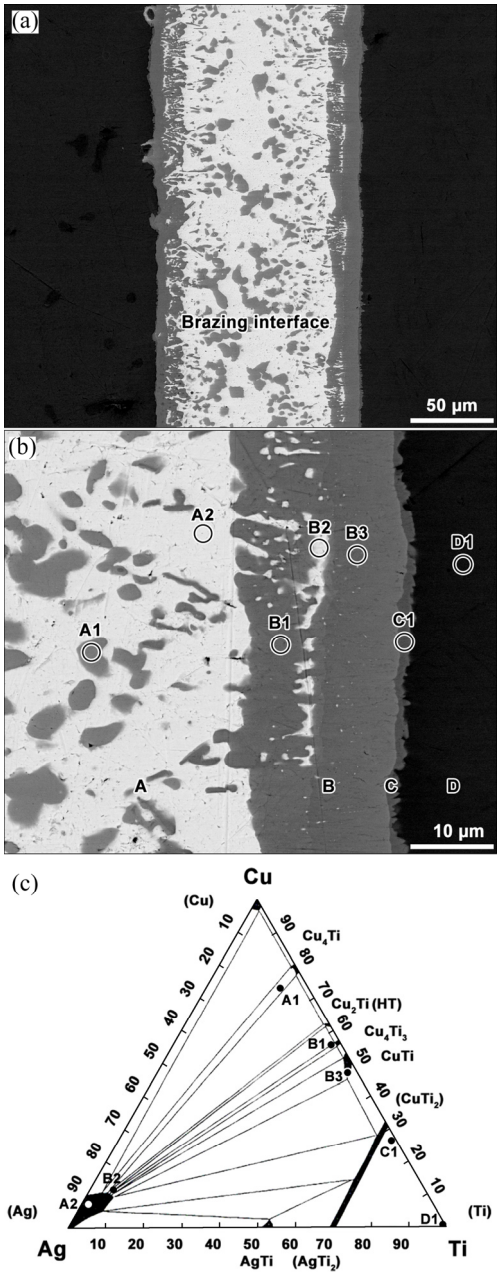

Fig. 3 BSE images of Ti/AgCu/Ti brazed joints showing global view (a), microstructure of brazing interface (b), and isothermal section of Ag−Cu−Ti phase diagram at 700 °C (c) [35]

Table 4 Chemical composition of zones shown in Fig. 3(b)

Layer	Zone	Composition/at.%			Possible phase
		Ag	Ti	Cu	
A	A1	7.4	20.3	72.3	Cu_4Ti
	A2	90.5	2.2	7.3	(Ag)
B	B1	2.0	42.4	55.6	Cu_4Ti_3
	B2	82.3	7.1	10.6	(Ag)
	B3	2.5	50.4	47.1	CuTi
C	C1	1.6	72.9	25.5	$CuTi_2$
D	D1	0.2	99.4	0.4	α-Ti

EDS analysis and the Ag−Cu−Ti phase diagram presented in Fig. 3(c), it could be assumed that Zone A1 should be mainly composed of Cu_4Ti, while Zone A2 should consist of (Ag). Layer B is about 20 μm, and should be essentially composed of Cu_4Ti_3 and CuTi, in addition to a smaller amount of (Ag). It can be observed from Fig. 3, CuTi (Zone B3), which is the Ti-richer phase in Layer B, is detected closer to the cp Ti sample, while the Cu- and Ag-richer phases, Cu_4Ti_3 and (Ag), i.e., Zones B1 and B2, respectively, are essentially detected closer to the central zone of the interface. Layer C is a continuous thin sheath, less than 3 μm in thickness, essentially composed of Ti and Cu and should consist of $CuTi_2$. It is obvious that in comparison to Layer A, Layers B and C, which are formed closer to the cp Ti sample, are richer in Cu and Ti. KVRYAN et al [27] reported that Ti atoms, which are diffusion from the cp Ti samples towards the interface, will react preferentially with Cu atoms from the braze, causing most of Ag to be segregated towards the central zone of the interface. Layer D is a narrow diffusion layer (in Fig. 3(b)), where small amounts of Cu and Ag are detected. Diffusion Layer D extends no more than 10 μm into the base cp Ti samples and should consist of α-Ti. Thus, the layered microstructure of the Ti/AgCu/Ti brazed joint interface could consist of Cu_4Ti+(Ag) (Layer A)/Cu_4Ti_3+(Ag)+CuTi (Layer B)/$CuTi_2$ (Layer C)/α-Ti (Layer D), sequentially from the central zone of the interface towards the cp Ti samples.

Most of phases presumably formed in Ti/AgCu/Ti brazed joints were also reported when similar brazing systems were studied. For instance, ANDRIEUX et al [44] analysed the existing reactions between Ti and Ag−Cu eutectic alloy at

790 °C in order to evaluate the extension and composition of the reaction zones formed at the interface. A layered reaction zone consisting sequentially of α-Ti/Ti_2Cu/TiCu/Ti_3Cu_4/$TiCu_4$ was observed near the Ti sample. LEE et al [18] joined cp Ti to stainless steel at 810 °C, using AgCu eutectic filler foil and reported the formation of a multilayered interface consisting essentially of (Ti)/Ti_2Cu/TiCu/(Ag)/TiFe, sequentially formed the cp Ti sample towards stainless steel. GANJEH et al [45] studied the effect of processing parameters, with time and temperature, on microstructure and mechanical properties of the Ti brazed joints using AgCuZnCd brazing alloy and found that the brazed interfaces consisted mostly of β-Ti and Ti_2Cu and Ag-rich phases, for joining at 850 and 870 °C, with dwelling stages of 10 and 20 min.

3.2 Electrochemical behaviour

3.2.1 Corroded Ti/TiCuNi/Ti joints

SEM images did not exhibit any visible preferential dissolution at the brazing interface of the Ti/TiCuNi/Ti joints (Fig. 4). Correspondingly, EDS analysis did not reveal any noticeable difference on the composition obtained before (Table 2) and after potentiodynamic polarization tests (Table 5). These results suggest that the intermetallics (independently of their nature) presented in the interface did not create a significant micro-galvanic effect.

Table 5 Chemical composition of different zones shown in Fig. 4(b) (at.%)

Zone	Ni	Ti	Cu
1	0.5	98.5	1.0
2	6.5	89.3	4.2
3	10.4	69.3	20.3

3.2.2 Corroded Ti/Ag/Ti joints

Figure 5 shows SEM images of the Ti/Ag/Ti interface after the potentiodynamic polarization tests and Table 6 presents the respective chemical compositions of the zones indicated in Fig. 5(b). It is possible to observe that there was a preferential dissolution around the Ag-rich phases marked as Zones 2a and 2b in Fig. 5(b).

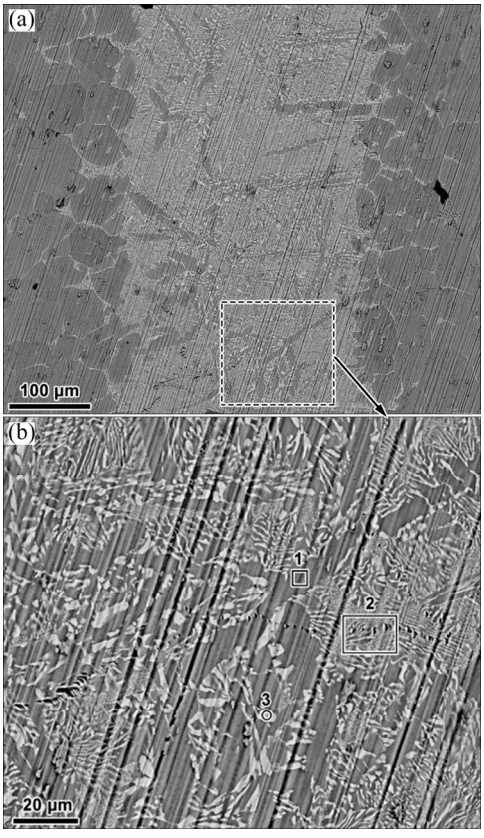

Fig. 4 BSE images of Ti/TiCuNi/Ti brazed joints corroded surface: (a) Global view; (b) Microstructure of brazing interface

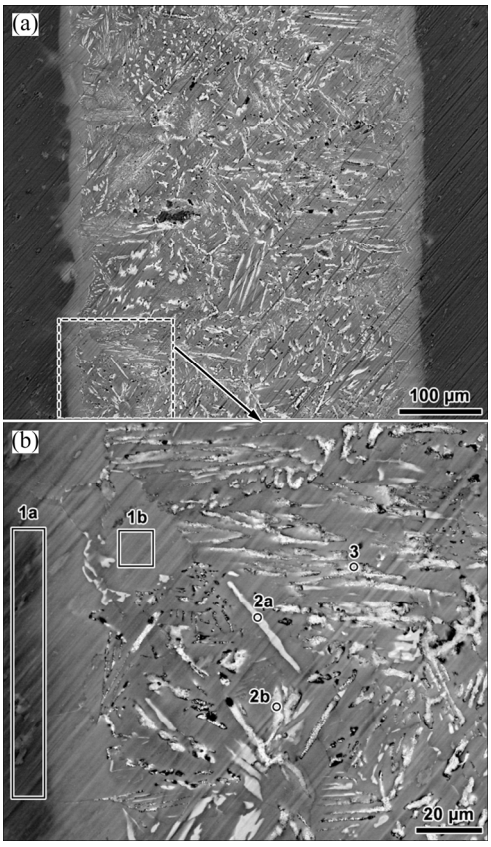

Fig. 5 BSE images of corroded surface on Ti/Ag/Ti brazed joints: (a) Global view; (b) Magnification of brazing interface

Table 6 Chemical composition of different zones shown in Fig. 5(b) (at.%)

Zone	Ti	O	Ag	Cl	P
1a	65.2	34.8	–	–	–
1b	55.8	38.1	6.1	–	–
2a	50.0	31.8	18.2	–	–
2b	31.3	41.3	26.1	1.3	–
3	37.4	36.1	24.4	0.8	1.3

ZAMBRANO CARRULLO et al [46] processed Ti−Ag alloys by powder metallurgy using either blended elemental powders or mechanical alloying, and compared their corrosion behaviour with cp Ti. They showed that Ti−Ag alloys produced by blended elemental route presented similar corrosion behaviour to cp Ti. On the other hand, due to the presence of the intermetallics (Ti_2Ag), the alloys produced by mechanical alloying presented reduced corrosion resistance due to the preferential dissolution in the periphery of the intermetallics. LEI et al [47] studied the influence of Ag content on the corrosion behaviour of Ti−Ag alloys obtained by powder metallurgy. They highlighted the nobler electrochemical behaviour of Ti−Ag alloys, compared with cp Ti, associated with the addition of nobler Ag element, nevertheless, they reported that inhomogeneous distribution of Ti_2Ag intermetallic compounds resulted in formation of more pores on the surfaces causing crevice corrosion and localized breakdown of the passive layer.

3.2.3 Corroded Ti/AgCu/Ti joints

Figure 6 shows SEM images after the potentiodynamic polarization tests for the interface obtained by brazing using AgCu filler and Table 7 presents the chemical composition of Zone 1 indicated in Fig. 6(b), which is mainly composed of AgCl. According to Ref. [18], in the absence of an intermediate layer of Ag, galvanic corrosion essentially occurs in the Ag-rich phases. EDS analysis suggests that the corrosion products were probably AgCl which were highly accumulated in this zone. ROCHA et al [29] reported that the presence of Cl^- in the electrolyte played an important role in the corrosion behaviour of glass-ceramic/Ti joints brazed by AgCuTi filler, since the reaction of Ag with Cl formed an adherent layer on the corroded surface. On the other hand, PAIVA and BARBOSA [28] showed that a high amount of Cu and Cl and a relatively low amount of Ag induced an increase in the corrosion rate of Al_2O_3/AgCuTi/Ti brazed joints. Moreover, Cu in contact with electrolytes rich in Cl^- ions formed soluble complex films, which corroded actively. However, in the present system, the amount of Cu-free to form soluble complex films was very low, thus the formation of these films was probably inhibited.

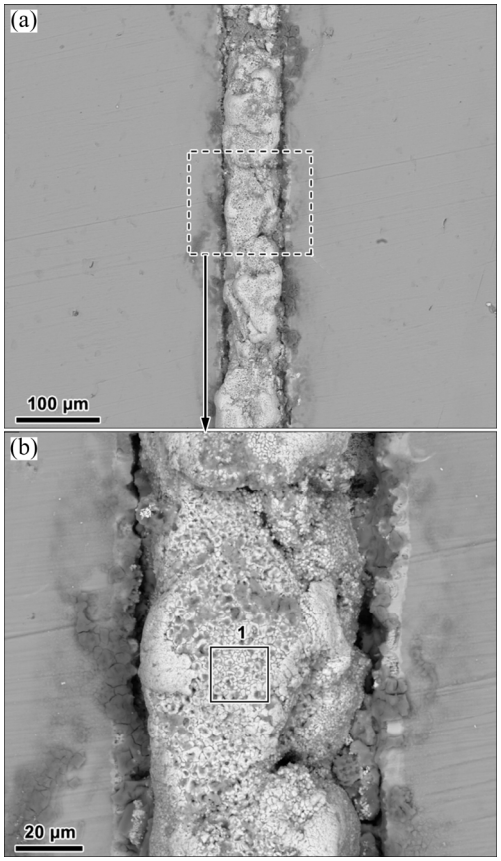

Fig. 6 BSE images of corroded surface on Ti/AgCu/Ti brazed joints: (a) Global view; (b) Magnification of brazing interface

Table 7 Chemical composition of Zone 1 shown in Fig. 6(b) (at.%)

Ag	Ti	Cu	Cl	P	O
30.6	1.9	8.8	25.3	0.6	32.8

3.2.4 Polarization behaviour

Representative potentiodynamic polarization curves of joints and cp Ti, used as control group, in PBS electrolyte at 37 °C are presented in Fig. 7. The electrochemical parameters taken from potentiodynamic polarization curves are given in Table 8. Similar results were obtained from potentiodynamic polarization curves for cp Ti and

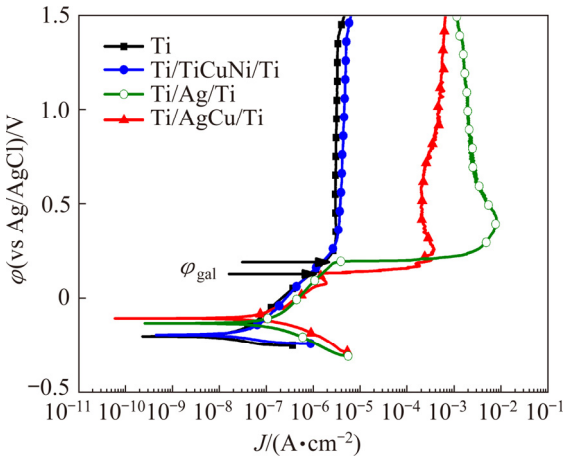

Fig. 7 Representative potentiodynamic polarization curves for all brazing interfaces together with cp Ti in PBS solution at 37 °C

Ti/TiCuNi/Ti joints, where a well-defined passivation plateau was observed, revealing a similar tendency to form a passive film. The passivation plateau started around 0.25 V (vs Ag/AgCl) leading to a passivation current density of about 2.5 μA/cm^2. Ti/TiCuNi/Ti joints presented a very similar behaviour to cp Ti control group, showing that the presence of the (Cu,Ni)Ti_2 intermetallic formed at the joint interface did not influence negatively the good corrosion behaviour of cp Ti. Thus, it is possible to state that a stable passive film was formed on Ti/TiCuNi/Ti brazed joints. These results are in accordance with Ref. [34], where no inferior electrochemical effect was observed on the behaviour of Ti−B_4C composites when joined with the same TiCuNi filler. LEE and LEE [17] produced Ti6Al4V brazed joints using Zr−Ti−Ni−Cu−Be filler and showed that when there was no segregated intermetallic phase at the brazing interface, the polarization behaviour of the joint was almost comparable to that of the Ti6Al4V. Therefore, based on the polarization curves (Fig. 7), SEM images (Fig. 4), and the EDS analysis (Table 5), it can be inferred that the interface obtained on the Ti/TiCuNi/Ti joints did not deteriorate the stability of the passive film and no localized corrosion was observed.

In contrast to the Ti/TiCuNi/Ti joints, the potentiodynamic polarization curves of Ti/Ag/Ti and Ti/AgCu/Ti joints are characterized by three stages on the anodic domain. In the first stage, the current densities increased with the applied potential, mostly due to the occurrence of corrosion, which was dominated by galvanic corrosion of Ag-rich regions in the joints (Figs. 5 and 6). The following stage presented an abrupt increase of current densities at potential values (φ_{gal}) of around 0.19 and 0.13 V (vs Ag/AgCl) for Ti/Ag/Ti and Ti/AgCu/Ti, respectively. In this stage, the formation and growth of micro-galvanic cells is likely to occur between Ag-rich zones and the base material or CuTi intermetallics. Finally, in the third stage, nearly constant current density values were reached where the galvanic corrosion products can make a blockade effect leading to a decrement of current densities [18]. Thus, it was possible to observe that both Ag and AgCu brazing fillers led to interfaces that accelerated the corrosion process (i.e. higher J_{corr} values) when compared with TiCuNi brazing filler. Furthermore, the polarization resistances of Ti/Ag/Ti and Ti/AgCu/Ti joints were much lower than that of Ti/TiCuNi/Ti joints.

Regarding Ti/Ag/Ti joints, based on the SEM images (Fig. 5), the EDS analyses (Table 6), and the potentiodynamic polarization curves (Fig. 7), it can be stated that the periphery of the TiAg and Ti_2Ag phases was dissolved preferentially at the testing conditions, most probably due to the galvanic coupling. Moreover, Ag has a strong affinity to react with Cl^- present in the electrolyte resulted in the formation of AgCl [28] (Table 6). On the other hand, in the case of Ti/AgCu/Ti joints, Ag is nobler than Cu, but due to its low solubility in AgCl, tends

Table 8 Open circuit potential (φ_{OCP}), corrosion potential ($\varphi_{i=0}$), galvanic potential (φ_{gal}), corrosion current density (J_{corr}), passivation current density (J_{pass}), and polarization resistance (R_p) values

Joint	φ_{OCP}(vs Ag/AgCl)/V	$\varphi_{(i=0)}$(vs Ag/AgCl)/V	φ_{gal}(vs Ag/AgCl)/V	J_{corr}/(10^{-8} A·cm^{-2})	J_{pass}/(μA·cm^{-2})	R_p/(MΩ·cm^2)
Ti	−0.07±0.10	−0.17±0.07	–	2.71±0.30	2.44±0.42	0.97±0.10
Ti/TiCuNi/Ti	−0.06±0.05	−0.20±0.03	–	6.54±2.93	3.49±1.95	0.54±0.16
Ti/Ag/Ti	−0.04±0.04	−0.15±0.02	0.19±0.02	13.71±0.78	–	0.19±0.01
Ti/AgCu/Ti	−0.07±0.07	−0.11±0.03	0.13±0.02	18.98±11.33	–	0.17±0.10

to passivate in Cl^--containing solutions, forming an adherent layer as it can be observed in Fig. 6. Thus, in this system, each possible phase may lead to a different corrosion behaviour, which leads to different anode and cathode areas originating micro-galvanic cells, that is also evidenced by the potentiodynamic polarization curves (Fig. 7). PAIVA and BARBOSA [28] and ROCHA et al [29] reported Ag-rich phases at the brazed glass-ceramic/AgCuTi/Ti interface. These Ag-rich phases reacted with the electrolyte Cl^- ions leading to the formation of a partially insoluble AgCl film. Moreover, a microstructure composed of a mixture of compounds rich either in Cu or in Ag led to galvanic corrosion since Cu-rich zones were less noble than Ag-based ones [28].

Depending on the nature of the intermetallic phases, they may act as anodic or cathodic sites relative to the base metal (cp Ti), which is critical for the initiation sites for galvanic corrosion. In this way, the potential differences between the anodic and cathodic sites are fundamental for the evaluation of the corrosion properties of the joint system. On a prosthesis having joined parts, the local potential differences can play an important role on the corrosion behaviour. Therefore, further studies should involve local electrochemical techniques, such as SKPFM technique used by KVRYAN et al [27] to identify the micro-galvanic cells on the stainless steel (316L) joints obtained by using Cu−Ag alloy filler, and they showed a clear difference in potential values between the Ag-rich and Cu-rich phases leading to galvanic corrosion.

Studies performed on Ti−Cu alloys showed that their corrosion behaviour is affected by the chemical composition and the microstructure of Ti−Cu intermetallics. PINA et al [48] processed Ti−xCu (x=3, 7.1 and 12 wt.%) alloys by conventional powder metallurgy. Independently, they reported hypoeutectoid microstructures and the presence of α-Ti and $CuTi_2$ phases, and showed that increasing the Cu content led to an improvement on the corrosion resistance of the alloy; however, this behaviour was just noticed up to a certain volume fraction of $CuTi_2$. On the other hand, OSÓRIO et al [49] reported that lamellar structures composed of intermetallics and α-Ti led to a galvanic coupling. However, this galvanic effect may be minimized by fine microstructures that modify the cathode/anode area ratio between the two different phases, leading to an improved corrosion resistance. WONG et al [50] identified laser-alloyed copper with titanium (Ti−xCu) intermetallics such as $CuTi_2$, CuTi, Cu_4Ti_3, and Cu_3Ti_2, together with α-Ti, and reported that all intermetallics were nobler than α-Ti. As Ti content increased, a reduced galvanic effect was observed between the phases and thus, the corrosion resistance increased. Among these intermetallics, $CuTi_2$ was expected to have the most stable oxide due to the highest Ti content. Similarly, studies on Ti−Ni alloys also showed the influence of the Ni content on the corrosion behaviour of the alloy. Among those, RYBALKA et al [51] concluded that when Ni content exceeded 5 wt.%, corrosion current increased with the increased amount of Ni. On the other hand, BARISION et al [52] showed that on the equimolar Ni−Ti alloy, Ni enhances the corrosion resistance of Ti due to the dissolution of Ni from the Ti_2Ni intermetallic compound.

The electrochemical behaviour of brazed joints is mostly characterized using conventional electrochemical techniques such as OCP monitoring, potentiodynamic polarization and/or cyclic polarization technique, and electrochemical impedance spectroscopy (EIS). However, these techniques allow to access only the global properties of the system, which is limited for fully understanding the localized corrosion processes as galvanic corrosion. Local electrochemical techniques, such as scanning vibrating electrode technique (SVET) and SKPFM should be performed in order to identify the localized anodic and cathodic activities at the brazed interfaces. Moreover, long-term immersion tests by monitoring the OCP and EIS can give a further understanding of the corrosion mechanisms at the brazed interfaces, particularly the preferential dissolution of the intermetallic phases. Besides, the influence of the corrosive environment on the mechanical properties should be fully understood.

4 Conclusions

(1) The interfacial microstructure of Ti/TiCuNi/Ti brazed joints could be described as α-Ti diffusion zone/α-Ti + $(Cu,Ni)Ti_2$ + lamelar (α-Ti + $(Cu,Ni)Ti_2$)/α-Ti diffusion zone.

(2) The interfacial microstructure of Ti/Ag/Ti brazed joints could be described as α-Ti diffusion layer/TiAg+Ti_2Ag+α-Ti/α-Ti diffusion layer.

(3) The interfacial microstructure of Ti/AgCu/Ti brazed joints could be described as α-Ti diffusion layer/Cu_4Ti + (Ag)/Cu_4Ti_3 + (Ag) + CuTi /$CuTi_2$/α-Ti diffusion layer.

(4) The corrosion behaviour of Ti brazed joints is governed by the phases formed at the joint interface.

(5) The intermetallic phases formed by TiCuNi brazing alloy did not deteriorate the good corrosion behaviour of the base material.

(6) When either AgCu or Ag fillers were used, potentiodynamic polarization tests and corroded microstructures revealed micro-galvanic corrosion.

Acknowledgments

This work was supported by Portuguese FCT, under the reference project UIDB/04436/2020 and M-ERA-NET/0001/2015 project. The authors would also like to acknowledge A. I. COSTA for her help on the experimental studies.

References

[1] AL-TAMIMI A A, PEACH C, FERNANDES P R, CSEK A, BARTOLO P J D S. Topology optimization to reduce the stress shielding effect for orthopedic applications [J]. Procedia CIRP, 2017, 65: 202−206.

[2] CHANG C T, YEH T Y, SHIUE R K, CHANG C S. Microstructural evolution of infrared brazed CP-Ti using Ti−Cu−Ni brazes [J]. Journal of Materials Science & Technology, 2011, 27(2): 131−138.

[3] NIINOMI M, NAKAI M. Titanium-based biomaterials for preventing stress shielding between implant devices and bone [J]. International Journal of Biomaterials, 2011, 2011: 10.

[4] KIKUCHI M, TAKADA Y, KIYOSUE S, YODA M, WOLDU M, CAI Z, OKUNO O, OKABE T . Mechanical properties and microstructures of cast Ti−Cu alloys [J]. Dental Materials, 2003, 19(3): 174−181.

[5] WANG R R, WELSCH G E. Joining titanium materials with tungsten inert gas welding, laser welding, and infrared brazing [J]. The Journal of Prosthetic Dentistry, 1995, 74(5): 521−530.

[6] WATANABE I, TOPHAM D S. Laser welding of cast titanium and dental alloys using argon shielding [J]. Journal of Prosthodontics, 2006, 15(2): 102−107.

[7] LI H X, HE P, LIN T S, PAN F, FENG J C, HUANG Y D. Microstructure and shear strength of reactive brazing joints of TiAl/Ni-based alloy [J]. Transactions of Nonferrous Metals Society of China, 2012, 22(2): 324–329.

[8] ZHAO D S, YAN J C, LIU Y J, JI Z S. Interfacial structure and mechanical properties of hot-roll bonded joints between titanium alloy and stainless steel using niobium interlayer [J]. Transactions of Nonferrous Metals Society of China, 2014, 24(9): 2839−2844.

[9] LI H, ZHANG C, LIU H B, LI M Q. Bonding interface characteristic and shear strength of diffusion bonded Ti-17 titanium alloy [J]. Transactions of Nonferrous Metals Society of China, 2015, 25(1): 80–87.

[10] DENG Y H, GUAN Q, TAO J. Effect of heating time on bonding interface, atom diffusion and mechanical properties of dissimilar titanium joints produced by thermal self-compressing bonding [J]. Transactions of Nonferrous Metals Society of China, 2018, 28(4): 662–668.

[11] NUÑEZ-PANTOJA J M C, VAZ L G, NÓBILO M A A, HENRIQUES G E P, MESQUITA M F. Effects of laser-weld joint opening size on fatigue strength of Ti−6Al−4V structures with several diameters [J]. Journal of Oral Rehabilitation, 2011, 38(3): 196−201.

[12] NUÑEZ PANTOJA J M C, FARINA A P, VAZ L G, CONSANI R L X, NÓBILO M A D A, MESQUITA M F. Fatigue strength: Effect of welding type and joint design executed in Ti−6Al−4V structures [J]. Gerodontology, 2012, 29(2): e1005−e1010.

[13] NUÑEZ-PANTOJA J M C, VAZ L G, NÓBILO M A D A. Fatigue performance of joints executed in pure titanium structures with several diameters [J]. Dental Materials Journal, 2011, 30(6): 887−893.

[14] BALASUBRAMANIAN M, JAYABALAN V, BALASUBRAMANIAN V. Modeling corrosion behavior of gas tungsten arc welded titanium alloy [J]. Transactions of Nonferrous Metals Society of China, 2007, 17(4): 676−680.

[15] CHUNG T, KIM J, BANG J, RHEE B, NAM D. Microstructures of brazing zone between titanium alloy and stainless steel using various filler metals [J]. Transactions of Nonferrous Metals Society of China, 2012, 22(S3): s639−s644.

[16] WAY M, WILLINGHAM J, GOODALL R. Brazing filler metals [J]. International Materials Reviews, 2019, 0(0): 1−29.

[17] LEE M K, LEE J G. Mechanical and corrosion properties of Ti−6Al−4V alloy joints brazed with a low-melting-point 62.7Zr−11.0Ti−13.2Cu−9.8Ni−3.3Be amorphous filler metal [J]. Materials Characterization, 2013, 81: 19−27.

[18] LEE M K, PARK J J, LEE J G, RHEE B. Phase-dependent corrosion of titanium-to-stainless steel joints brazed by Ag−Cu eutectic alloy filler and Ag interlayer[J]. Journal of Nuclear Materials, 2013, 439(1−3): 168−173.

[19] ELREFAEY A, TILLMANN W. Correlation between microstructure, mechanical properties, and brazing temperature of steel to titanium joint [J]. Journal of Alloys and Compounds, 2009, 487(1−2): 639−645.

[20] HAN W P, WAN M, ZHAO R. Vacuum brazing of the ultrathin-walled structure using particulate-reinforced composite filler metal: Microstructural evolution and mechanical properties [J]. Journal of Alloys and Compounds, 2019, 805: 638−647.

[21] HAN G H, BIAN H, ZHAO H Y, SONG XG, LI Y, LIU D, CAO J, FENG J C. Interfacial microstructure and mechanical properties of TZM alloy and ZrC particle reinforced tungsten composite joint brazed using Ti−61Ni filler [J]. Journal of Alloys and Compounds, 2018, 747: 266−275.

[22] XIA C, SUN W, ZHOU Y, XU X. Thermal fatigue damage and residual mechanical properties of W−Cu/Ag−Cu/

1Cr18Ni9 brazed joint [J]. Journal of Alloys and Compounds, 2018, 741: 155−160.

[23] SONG X, BEN B, HU S, FENG J, TANG D. Vacuum brazing high Nb-containing TiAl alloy to Ti60 alloy using Ti−28Ni eutectic brazing alloy [J]. Journal of Alloys and Compounds, 2017, 692: 485−491.

[24] LI P, LEI Z, ZHANG X, LIU J, CHEN Y. Effects of laser power on the interfacial intermetallic compounds and mechanical properties of dual-spot laser welded–brazed Ti/Al butt joint [J]. Optics and Laser Technology, 2020, 124: 105987.

[25] MANDAL S, RAY A K, RAY A K. Correlation between the mechanical properties and the microstructural behaviour of Al_2O_3−(Ag−Cu−Ti) brazed joints [J]. Materials Science and Engineering A, 2004, 383(2): 235−244.

[26] QIU Q, WANG Y, YANG Z, HU X, WANG D. Microstructure and mechanical properties of TiAl alloy joints vacuum brazed with Ti−Zr−Ni−Cu brazing powder without and with Mo additive [J]. Materials and Design, 2016, 90: 650−659.

[27] KVRYAN A, LIVINGSTON K, EFAW C M, KNORI K, JAQUES B J, DAVIS P H, BUTT D P, HURLEY M F. Microgalvanic corrosion behavior of Cu−Ag active braze alloys investigated with SKPFM [J]. Metals, 2016, 6(4): 91.

[28] PAIVA O C, BARBOSA M A. Brazing parameters determine the degradation and mechanical behaviour of alumina/ titanium brazed joints [J]. Journal of Materials Science, 2000, 35(5): 1165−1175.

[29] ROCHA L A, BARBOSA M A, PUERS R. Active metal brazing for joining glass-ceramic to titanium-a study on silver enrichment [J]. Journal of Materials Science: Materials in Medicine, 1995, 6(12): 835–838.

[30] KIM K H, LEE J G, LEE G J, PARK J J, LEE M K. Compositional effects of Zr-rich multi-component brazing alloys on the corrosion of Zr alloy joints [J]. Corrosion Science, 2014, 88: 328–336.

[31] ELREFAEY A, WOJARSKI L, TILLMANN W. Evaluation of corrosion performance of titanium/steel joint brazed by Cu-based filler metal [J]. Journal of Materials Engineering and Performance, 2012, 21(5): 707–713.

[32] BENEDETTI A, GAMBARO S, VALENZA F, FAIMALI M, COLLI M, HOSTASA J, DELUCCI M. Ag and AgCu as brazing materials for Ti6Al4V-Y3Al5O12 joints: Does ennoblement affect the galvanic behaviour in seawater? [J]. Electrochimica Acta, 2018, 283: 155–166.

[33] LEE J G, CHOI Y H, LEE J K, LEE G J, LEE M K, RHEE C K. Low-temperature brazing of titanium by the application of a Zr−Ti−Ni−Cu−Be bulk metallic glass (BMG) alloy as a filler [J]. Intermetallics, 2010, 18(1): 70−73.

[34] SOUSA J M, ALVES A C, TOPTAN F, ARIZA E, GUEDES A. Corrosion and tribocorrosion behavior of Ti−B4C composites joined with TiCuNi brazing alloy [J]. Journal of Materials Engineering and Performance, 2019, 28(8): 4972−4982.

[35] VILLARS P, PRINCE A, OKAMOTO H. Handbook of ternary alloy phase diagram [M]. Materials Park, Ohio: ASM International, 1995.

[36] LEE S J, WU S K, LIN R Y. Infrared joining of TiAl intermetallics using Ti−15Cu−15Ni foil-I. The microstructure morphologies of joint interface [J]. Acta Materialia, 1998, 46(4): 1283−1295.

[37] GOMES L, GUEDES A. Influence of the brazing filler on the microstructure of Ti6Al4V joints [J]. Microscopy and Microanalysis, 2016, 22: 40−41.

[38] SHIUE R K, WU S K, CHEN Y T. Strong bonding of infrared brazed α2-Ti3Al and Ti−6Al−4V using Ti−Cu−Ni fillers [J]. Intermetallics, 2010, 18: 107−114.

[39] MURRAY J L, BHANSALI K J. The Ag−Ti (silver−titanium) system [J]. Bulletin of Alloy Phase Diagrams, 1983, 4(2): 178−183.

[40] SHIUE R K, WU S K, CHEN S Y. Infrared brazing of TiAl intermetallic using pure silver [J]. Intermetallics, 2004, 12(7−9): 929−936.

[41] DENG Y Q, SHENG G M, HUANG Z H, FAN L Z. Microstructure and mechanical properties of diffusion bonded titanium/304 stainless steel joint with pure Ag interlayer [J]. Science and Technology of Welding and Joining, 2013, 18: 143−146.

[42] WANG T, ZHANG B, WANG H, FENG J. Microstructures and mechanical properties of electron beam-welded titanium-steel joints with vanadium, nickel, copper and silver filler metals [J]. Journal of Materials Engineering and Performance, 2014, 23(4): 1498−1504.

[43] YU L Q, MO D F, LI X, FANG Y J, JIANG X S, ZENG Z J, CHEN J L, GONG H M. Microstructure and mechanical properties of electron beam welded joints of titanium alloy and Kovar alloy with copper or silver interlayer [J]. Materials Research Express, 2019, 6(11): 116508.

[44] ANDRIEUX J, DEZELLUS O, BOSSELET F, VIALA J C. Low-temperature interface reaction between titanium and the eutectic silver-copper brazing alloy [J]. Journal of Phase Equilibria and Diffusion, 2009, 30(1): 40−45.

[45] GANJEH E, SARKHOSH H, KHORSAND H, SABET H, DEHKORDI E H, GHAFFARI M. Evaluate of braze joint strength and microstructure characterize of titanium-CP with Ag-based filler alloy [J]. Materials and Design, 2012, 39: 33−41.

[46] ZAMBRANO CARRULLO J C , DALMAU BORRÁS A, AMIGÓ BORRÁS V, NAVARRO-LABOULAIS J, PEREIRA FALCÓN J C. Electrochemical corrosion behavior and mechanical properties of Ti–Ag biomedical alloys obtained by two powder metallurgy processing routes [J]. Journal Mechanical Behavior Biomedical Materials, 2020, 112: 104063.

[47] LEI Z, ZHANG H, ZHANG E, YOU J, MA X, BAI X, Antibacterial activities and biocompatibilities of Ti−Ag alloys prepared by spark plasma sintering and acid etching [J]. Materials Science Engineering C, 2018, 92: 121−131.

[48] PINA V G, AMIGÓ V, MUÑOZ A I. Microstructural, electrochemical and tribo-electrochemical characterisation of titanium-copper biomedical alloys [J]. Corrosion Science, 2016, 109: 115–125.

[49] OSÓRIO W R, FREIRE C M, CARAM R, GARCIA A. The role of Cu-based intermetallics on the pitting corrosion behavior of Sn−Cu, Ti−Cu and Al−Cu alloys [J]. Electrochimica Acta, 2012, 77: 189−197.

[50] WONG P K, KWOK C T, MAN H C, CHENG F T.

Corrosion behavior of laser-alloyed copper with titanium fabricated by high power diode laser [J]. Corrosion Science, 2012, 57: 228−240.

[51] RYBALKA K V, BEKETAEVA L A, BUKHAN'KO N G, DAVYDOV A D. Dependence of corrosion current on the composition of titanium-nickel alloy in NaCl solution [J]. Russian Journal of Electrochemistry, 2014, 50(12): 1149−1156.

[52] BARISON S, CATTARIN S, DAOLIO S, MUSIANI M, TUISSI A. Characterisation of surface oxidation of nickel-titanium alloy by ion-beam and electrochemical techniques [J]. Electrochimica Acta, 2004, 50(1): 11−18.

TiCuNi、AgCu 和 Ag 钎料真空钎焊钛接头的电化学响应

C. MARINHO[1], F. TOPTAN[1,2], A. GUEDES[1,3], A. C. ALVES[1]

1. CMEMS-UMinho, Center of MicroElectroMechanical Systems, University of Minho, Guimarães, Portugal;
2. IBTN/Euro, European Branch of the Institute of Biomaterials, Tribocorrosion and Nanomedicine, Department of Mechanical Engineering, University of Minho, Guimarães, Portugal;
3. Department of Mechanical Engineering, University of Minho, Guimarães, Portugal

摘　要：接头的性质取决于界面形成相的性质、分布和形态。钎焊接头的力学性能有详细的文献记录，而对其电化学行为的研究却较少。因此，本研究的主要目的是了解用 TiCuNi、AgCu 共熔合金和 Ag 钎料钎焊工业纯钛接头界面处形成的相对其腐蚀行为的影响。在磷酸盐缓冲电解液中进行 37 °C 下的开路电位和动电位极化实验，研究钛接头的电化学行为。结果表明，含 Ag 钎料对界面形成的富银相及钛相和工业纯钛间的微电偶腐蚀具有敏感性。然而，当使用 TiCuNi 钎料钎焊时，接头和母材之间没有显著差异。

关键词：生物材料；钛；连接；钎焊合金；界面；显微组织；腐蚀

(Edited by Xiang-qun LI)